Preemptive CD20+ B cell depletion attenuates cardiac allograft vasculopathy in cyclosporine-treated monkeys

Shahrooz S. Kelishadi,[1,2] Agnes M. Azimzadeh,[1] Tianshu Zhang,[1,2] Tiffany Stoddard,[1,2] Emily Welty,[1] Christopher Avon,[1] Mitch Higuchi,[1] Amal Laaris,[1,2] Xiang-Fei Cheng,[1] Christine McMahon,[3] and Richard N. Pierson III[1,2]

[1]Department of Surgery, University of Maryland School of Medicine, Baltimore. [2]VA Maryland Health Care System, Baltimore. [3]Department of Pathology, University of Maryland School of Medicine.

Chronic rejection currently limits the long-term efficacy of clinical transplantation. Although B cells have recently been shown to play a pivotal role in the induction of alloimmunity and are being targeted in other transplant contexts, the efficacy of preemptive B cell depletion to modulate alloimmunity or attenuate cardiac allograft vasculopathy (CAV) (classic chronic rejection lesions found in transplanted hearts) in a translational model has not previously been described. We report here that the CD20-specific antibody (αCD20) rituximab depleted CD20+ B cells in peripheral blood, secondary lymphoid organs, and the graft in cynomolgus monkey recipients of heterotopic cardiac allografts. Furthermore, CD20+ B cell depletion therapy combined with the calcineurin inhibitor cyclosporine A (CsA) prolonged median primary graft survival relative to treatment with αCD20 or CsA alone. In animals treated with both αCD20 and CsA that achieved efficient B cell depletion, alloantibody production was substantially inhibited and the CAV severity score was markedly reduced. We conclude therefore that efficient preemptive depletion of CD20+ B cells is effective in a preclinical model to modulate pathogenic alloimmunity and to attenuate chronic rejection when used in conjunction with a conventional clinical immunosuppressant. This study suggests that use of this treatment combination may improve the efficacy of transplantation in the clinic.

Introduction

The majority of human allograft recipients develop clinically significant chronic rejection, with incidence and severity increasing steadily over time after transplant. For example, over 50% of human cardiac allograft recipients and 80% of lung recipients exhibit chronic rejection within 10 years. Recent additions to the clinical immunosuppressive armamentarium, such as blocking (1) or depleting antibodies (2) and pharmacologic inhibitors (3), have had little appreciable impact on this phenomenon (4–6).

The causes of chronic rejection remain incompletely understood. The classic chronic rejection lesions found in heart (cardiac allograft vasculopathy [CAV]), lung (obliterative bronchiolitis), liver (vanishing bile duct syndrome), and renal (chronic allograft nephropathy) allografts are often temporally associated with detection of anti-donor antibodies, implicating alloantibody as an effector mechanism. Animal models (7–10) and clinical data (11–13) consistently implicate T cell–mediated immunity in the elicited alloantibody response. Thus the current consensus paradigm for chronic rejection holds that T cell–mediated adaptive immunity to alloantigens amplifies innate immune activation initiated by donor brain death and organ ischemia/reperfusion. Influenced in part by the intensity of innate immune activation, T cells propagate pathogenic vascular remodeling and sustain alloantigen-specific chronic inflammation in the transplanted organ. Under the influence of Th cell costimulation, allospecific B cells expand and undergo affinity maturation events and are principally involved in the effector phase of chronic rejection by giving rise to pathogenic anti-donor alloantibody. Consequently, the majority of work in the field has focused on identifying and targeting upstream T cell pathways, including T cell costimulatory molecules and associated intracellular signaling pathways essential for efficient provision to B cells of T cell "help."
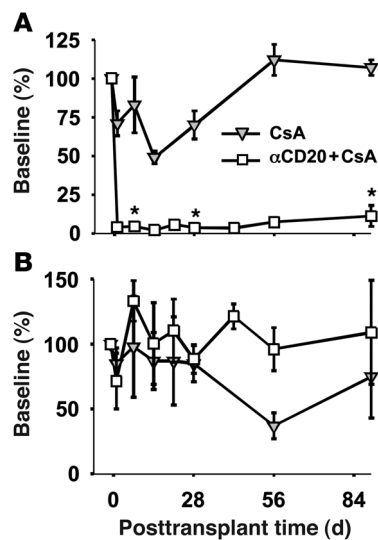
However, when B cells are deficient in antigen-presenting function due to restricted absence of MHC class II expression, primary cardiac allograft survival is significantly prolonged, an effect that is unanticipated by the conventional allograft rejection paradigm (14). In primate islet allograft recipients, addition of rituximab to preemptively deplete B cells at the time of transplant facilitated prevalent long-term islet allograft survival in cynomolgus monkeys treated with antithymocyte globulin induction followed by rapamycin monotherapy (15). These observations suggest that B cells exert pivotal, nonredundant influence in the immune response to an allograft at a point proximal to alloantibody elaboration, as recently described with respect to autoimmunity (16).

Here we report that, in a preclinical cynomolgus monkey heart allograft model, preemptive CD20+ B cell depletion around the time of transplant modulates acute rejection of an organ allograft, attenuates alloantibody elaboration, and inhibits CAV in the context of a clinically relevant calcineurin-based immunosuppressive regimen. These data demonstrate the potential value of preemptive B cell depletion as what we believe to be a novel adjunct to delaying or preventing chronic rejection after transplantation of the heart and perhaps other solid organs.

Figure 1

B cell depletion in blood after αCD20 therapy. Cardiac transplant recipients were treated with CsA alone or with additional αCD20 treatment (rituximab, 20 mg/kg; days −1, 7, 14, and 21). One animal (DJ3M5) exhibiting high T cell counts at day 14 in association with acute parvovirus infection was censored from this analysis. (**A**) Peripheral blood B cells are efficiently depleted for over 2 months after αCD20 treatment ends. Data include DJ4J7, in which recovery to 20%–40% was seen within 2 months (see Supplemental Figure 1). (**B**) T cell numbers in peripheral blood are not significantly affected by αCD20 treatment. Blood cell levels are expressed as percentage of baseline levels (mean ± SEM). *$P < 0.05$ for αCD20+CsA vs. CsA alone, noted only at time intervals after transplant when sufficient individual measurements were available to justify statistical analysis.

Results

αCD20 depletes peripheral B cells. Monkeys treated with rituximab in addition to cyclosporine A (CsA) (αCD20+CsA) exhibited greater than 90% B cell depletion in peripheral blood on the day after treatment. Depletion remained efficient in association with trough αCD20 levels (1 week following each dose) and generally persisted in peripheral blood through the 12-week follow-up period (Figure 1A). One animal (DJ4J7) displayed incomplete depletion of B cells in secondary lymphoid organs in response to the first dose of rituximab and also exhibited substantial recovery in circulating B cells (to 15% and 30% of baseline numbers at 2 and 3 months, respectively) (Supplemental Figure 1A; supplemental material available online with this article; doi:10.1172/JCI41861DS1). The explanation for less efficient and durable B cell depletion in DJ4J7 is unknown. Circulating B

cell depletion was not attributable to the heart transplant procedure or to calcineurin inhibitor treatment, since CsA-treated transplant recipients exhibited only a slight drop in B cells in the first weeks after transplant, with a return to baseline levels after 8 weeks.

As expected, no consistent differences were noted in peripheral blood absolute T cell numbers with αCD20 treatment (Figure 1B and Supplemental Figure 1B).

Immunohistochemistry consistently revealed efficient B cell depletion in spleen and LN associated with αCD20 treatment relative to CsA or no immunosuppression (Figure 2). Only DJ4J7 displayed significantly less efficient depletion in lymphoid organs than other animals. Partial recovery of B cells in spleen and LN by about 70 days after the last rituximab dose was consistently observed (Figure 2).

Treatment-related complications. B cell depletion was generally well tolerated, without clinical evidence of unusual susceptibility to infection despite omission of antiviral prophylaxis (15). Posttransplant lymphoproliferative disease and cytomegalovirus pneumonia, which are common with intense immunosuppression in macaque
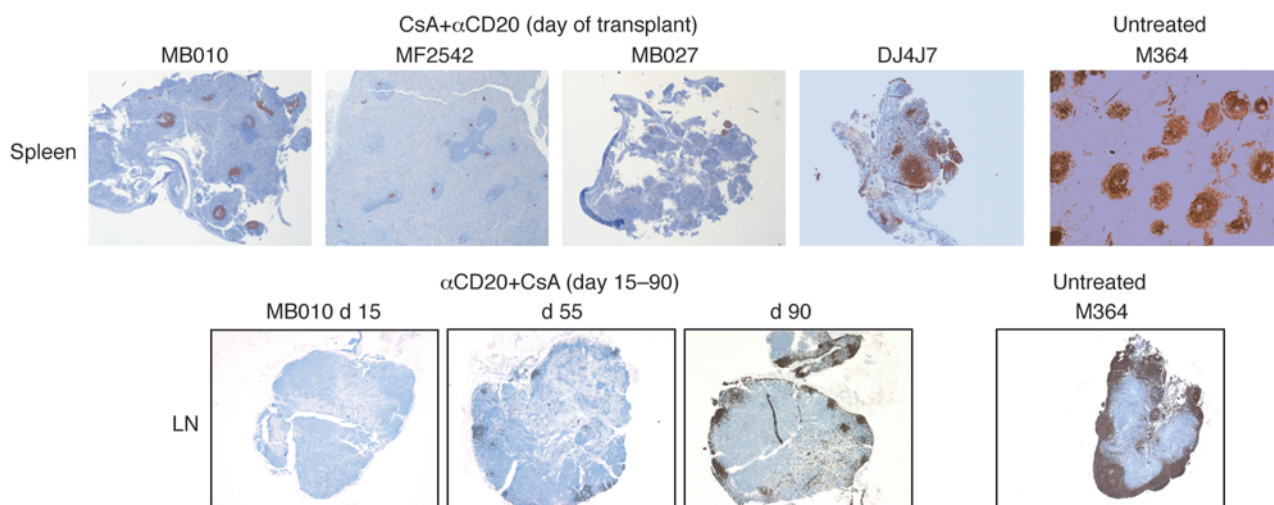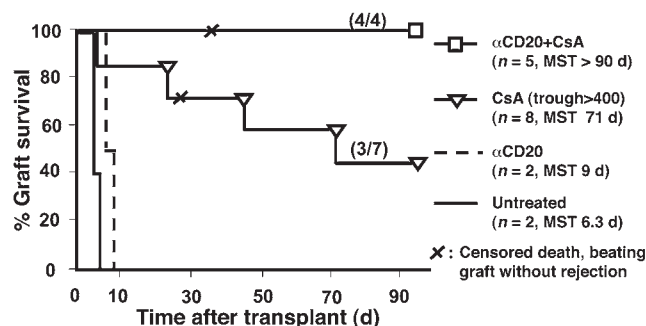

Figure 2

B cell depletion in lymphatic tissues after anti-CD20 therapy. Spleen and mesenteric LN from transplant recipients treated with αCD20+CsA reveal efficient B cell depletion in secondary lymphoid organs 1 day after treatment compared with untreated controls (shown at day 7) and CsA monotherapy (not shown). Monkey DJ4J7 only showed a partial response to αCD20 but also exhibited less durable B cell depletion in peripheral blood and graft. Partial recovery of B cell populations is observed in LN marginal zones (MB010) and splenic germinal centers (not shown) by day 90 after transplantation (~70 days after the last αCD20 treatment) in association with durable B cell depletion in peripheral blood and graft. Original magnification, ×25.

Figure 3
Primary graft survival by treatment regimen. Cynomolgus monkey recipients of MHC-mismatched heterotopic cardiac allografts were either not given immunosuppression (untreated, black line), given αCD20 alone (dashed line), or treated with daily CsA intramuscularly, titrated to achieve target trough blood levels of more than 400 ng/ml, as monotherapy (triangles) or with additional αCD20 (squares). Graft function was monitored by telemetric ECG and pressure waveforms, and clinical rejection was treated with steroids. CsA alone prolonged graft survival relative to no treatment ($P < 0.01$). Addition of αCD20 to CsA tended to prolong rejection-free primary graft survival ($P = 0.08$ vs. CsA alone). Numbers in parentheses indicate grafts without clinical rejection by 90 days/uncensored grafts at risk.

species, were not observed in any animal in this series. Mild anemia, marginal food intake, and peripheral edema were occasionally associated with daily intramuscular CsA injection, occurred with similar frequency with or without additional αCD20 treatment, and prompted early euthanasia of 1 CsA-treated animal on day 85 (M262). Three animals died with beating grafts prior to reaching the 90-day end point for the protocol. Two were censored from the graft survival analysis due to recipient death with a beating graft; these deaths were attributed to central line infection (MA029, CsA group, on day 26) and acute parvovirus infection (DJ3M5, αCD20+CsA group, on day 35), respectively. One recipient died of central line infection 3 days after steroids were administered to treat acute rejection (MA939, CsA group, on day 47).

Addition of anti-CD20 to CsA prolongs primary graft survival. As previously reported, in this model, monkeys reject cardiac allografts within 1 week in the absence of immunosuppressive treatment (untreated, $n = 5$, median survival time [MST], 6.5 ± 0.2 days; refs. 10, 17). Anti-CD20 alone yielded minimal prolongation of graft survival, to 8 and 9 days, respectively, in 2 recipients (Figure 3). Four of seven evaluable recipients treated with CsA monotherapy exhibited acute rejection before day 90. One graft failed due to acute graft rejection on day 7 before steroids could be initiated (Table 1); 3 others responded to treatment with methylprednisolone, with fever resolution and recovery of graft contractility and heart rate. In contrast, αCD20+CsA was associated with a strong trend toward reduced incidence of acute rejection within 90 days (0% vs. 57% with CsA alone; $P = 0.08$) and increased primary graft survival (median survival >90 days) relative to CsA alone (median 71 days, $P = 0.08$; Figure 3).

Effect of αCD20 on graft cellular infiltrate phenotype. Histological features of cardiac allograft rejection were quantified according to the clinical International Society of Heart and Lung Transplantation (ISHLT) scoring scale (18). Without immunosuppression or with αCD20 monotherapy, failed grafts revealed hemorrhagic necrosis at explant between days 6 and 9 (Table 1). With CsA monotherapy,

a substantial proportion of the protocol biopsies (10 of 21) and the majority of clinically well-functioning grafts (6 of 7) displayed moderate-to-severe cellular rejection within the first 2 months and at explant (6 of 8) (Supplemental Figure 3 and Table 1). In contrast, with additional αCD20, only 1 of 12 evaluable biopsies in 5 recipients displayed an ISHLT score greater than 1 during the first 2 months. Explant ISHLT rejection scores with additional CD20 depletion revealed absent or mild graft leukocyte infiltration (ISHLT score 0–1) in all but the one subject that exhibited incomplete initial B cell depletion and partial recovery of peripheral blood B cells after 2 months: DJ4J7 had ISHLT scores of 1 at days 14 and 28, and 2 at explant on day 91.

Intragraft B cell–rich cellular infiltrates were prominent at the time of explant in recipients receiving no immunosuppression (B cell score: 3.8 ± 0.2) (Table 1). B cells were sparse in the 2 rejected grafts explanted from anti-CD20 monotherapy animals at days 8 and 9 (B cell score: 0.5 ± 0.5). With CsA monotherapy, moderate B cell infiltrates were consistently observed in tissue biopsies collected after 2, 4, or 8 weeks after transplantation (B cell scores ranged from 1.8 to 2.4) and were moderate to severe at protocol explant around day 90 (mean B cell score: 3.2 ± 0.5, range 1.5–4) (Figure 4). In contrast, B cells were rarely found in the graft of animals treated with αCD20 antibody in protocol biopsies obtained between weeks 2 and 8 (B cells scores 0-0.2), and B cell infiltration was relatively mild at the time of protocol explant at 3 months (B cell score 1 ± 0.7; $P = 0.067$ vs. CsA alone, including DJ4J7) (Table 1 and Figure 4). Although DJ4J7's explanted graft contained smaller B cell clusters than most CsA monotherapy–treated grafts, the B cell score (3) reflected relatively intense B cell infiltration (Supplemental Figure 2).

Effect of αCD20 on CAV and anti-donor alloantibody. CAV chronic rejection lesions were significantly less severe 3 months after transplantation in association with additional CD20 depletion (mean CAV score 0.23 ± 0.13; range 0.1–0.36) relative to CsA alone (1.90 ± 0.43; range 1.5–2.45; $P = 0.01$) (Figure 5). CAV was mild in DJ4J7 (CAV score 0.33) in the context of initially incomplete and subsequently less durable B cell depletion. Five of the seven evaluable CsA monotherapy animals (1 recipient lacked viable donor lymphocytes) consistently elaborated anti-donor IgM alloantibody (71% incidence); in 3 of 7 (43%), anti-donor IgG alloantibodies were also detected. In contrast, in only 1 of the 5 CsA+αCD20 recipients were anti-donor IgM and IgG alloantibody consistently detected (DJ4J7; 20% incidence), a trend ($P = 0.24$) that approaches statistical significance for IgM ($P = 0.06$) when DJ4J7 is omitted as an incomplete rituximab responder (Figure 6).

Effect of αCD20 on B and T cell gene expression within the graft. CD20 mRNA expression tended to be decreased in CsA monotherapy grafts at graft explant relative to hearts acutely rejecting in the absence of immunosuppression ($P = 0.12$; Figure 7A). When αCD20 treatment was associated with efficient, durable B cell depletion, there was a statistically significant decrease in CD20 mRNA expression between untreated controls and αCD20+CsA ($P < 0.04$ without DJ4J7); failure to attenuate CD20 message in DJ4J7 corroborates the immunohistochemical (IHC) finding of B cell infiltrates in that graft. Expression of PAX5, a transcription factor expressed exclusively in the B lymphoid lineage, mirrored that of CD20 (Supplemental Figure 4). This result corroborates the CD20 expression result, indicating that B cells were not numerous in αCD20-treated grafts when B cell depletion was efficient, and specifically suggests that B cells with downmodulated CD20 had not infiltrated the graft (19). B cell–activating factor of the TNF

Table 1
Individual graft survival time and histological analysis at explant of monkey cardiac allografts treated with various regimens

Animal ID	1° survival[A] (d)	2° survival[B] (d)	ISHLT score[C]	CAV score[C]	B cell score[C]
Untreated					
M360	6		2	NA	4
M364	6		2	NA	4
M20	6.5		3	NA	4
M278	7		3	NA	3
M342	7		3	NA	4
Median	6.5		2.6 ± 0.5[D]	NA	3.8 ± 0.2
αCD20					
MDL41	9		3	NA	0
MDL1X	8		3	NA	1
Median	8.5		3 ± 0	NA	0.5 ± 0.5
CsA					
M162	7		3	NA	1
M9421	23	72	3	2.3	4
MA029	>26[E]		1[E]	0.7 [E]	3
MA939	44	47	1	1.5	2
M115	71	>92	3	2.5	2.5
M262	>85		2	1.6	1.5
MA049	>91		2	2.1	4
MA095	>89		2	1.5	4
Median	71		2.1 ± 0.8	1.9 ± 0.4	2.7 ± 0.4
αCD20+CsA					
DJ3M5	>35[E]		1[E]	0.1[E]	0
DJ4J7	>91		2	0.3	3
MF2542	>91		1	0.1	0
MB010	>96		1	0.4	1
MB027	>97		1	0.1	0
Median	>93		1.2 ± 0.4[F,G]	0.2 ± 0.1[H]	0.8 ± 0.6[F,G]

[A]1°: Primary graft survival time indicates the time at which the recipient was treated for graft rejection or at which a rejected graft was explanted (M162). Clinical rejection was treated with steroids in the CsA group. Time of survival preceded by "less than" symbol represents grafts beating at predetermined study end point (90 days) or at sacrifice before 90 days for animal health reasons. [B]2°: Secondary graft survival following initial rejection treatment. [C]ISHLT score: acute rejection score. B cell score: intensity of CD20+ cellular infiltrate, by IHC staining. Histologic scores determined as described in Methods. [D]Group histology statistics are expressed as mean ± SD for ISHLT and CAV scores and mean ± SEM for B cell score. [E]Animals that died with a beating graft before reaching the primary graft survival end point or 85 days were censored from the graft survival, ISHLT, and CAV analyses. [F]P < 0.05 vs. untreated group. [G]P < 0.05 vs. CsA group. [H]P < 0.001 vs. CsA group.

family (BAFF) (Figure 7A), a cytokine associated with B cell proliferation, and the costimulatory molecules CD80 (Figure 7A) and CD86 (data not shown) were significantly decreased in the graft at graft explant in association with peritransplant B cell depletion compared with untreated controls at explant (P = 0.02).

Analysis of selected T cell–associated genes in protocol graft biopsies confirmed ISHLT score and IHC findings that both CsA treatment and additional B cell depletion significantly attenuate T cell infiltrate intensity (CD3E; Figure 7B; P = 0.01) and show that its phenotype is altered (Figure 7, B and C) relative to grafts acutely rejecting without immunosuppression. However, relative to CsA alone, αCD20+CsA did not significantly modulate T cell activation (CD28, Figure 7B; and ICOS, not shown) or suppress Th1 cytokine gene expression (IFN-γ; Figure 7C). Only CsA alone

significantly attenuated IL-4 (Th2), whereas IL-17 was significantly decreased only with αCD20+CsA (Figure 7C); thus Th1/Th2 cytokine ratio was significantly lower only with CsA+αCD20 therapy versus untreated controls (IFN-γ/IL-4 ratio, P = 0.037). Although neither CsA monotherapy nor αCD20+CsA significantly altered expression of FOXP3 compared with unmodified acute rejection, the net ratio between expression of proinflammatory genes (IFN-γ+IL-17+TNF-α) or costimulatory genes (CD28+ICOS+CD80+CD86; calculations not shown) relative to *FOXP3* gene expression was significantly decreased with both CsA and αCD20+CsA therapies compared with acutely rejected grafts in recipients without immunosuppression (P = 0.016).

Antibody-dependent vascular complement deposition. Clinically significant anti-donor antibody elaboration might be undetectable in blood due to adsorption of antibody to the graft. To independently evaluate antibody-dependent complement activation on coronary vascular endothelium, vascular C4d deposition was measured in grafts explanted electively after day 85. In grafts from the CsA monotherapy group and from DJ4J7, C4d scores ranged between 1 and 2.5 (median 2), demonstrating significant complement deposition and showing that presence of alloantibody in blood is associated with significant complement activation in the graft. In the other 3 long-surviving, electively explanted grafts from the αCD20+CsA group, in which alloantibody was not detected in serum, C4d scores ranged between 0.5 and 1 (median 0.5) (Supplemental Figure 5). This finding demonstrates that perioperative "induction" B cell depletion is associated with reduced antibody-dependent complement activation within graft vasculature and confirms that additional B cell depletion around the time of transplant significantly inhibits elaboration of pathogenic antigraft immunity.

Discussion

For the past 4 decades, clinical transplant efficacy has improved markedly based on an expanding array of immunosuppressive agents, including antiinflammatory corticosteroids, antimitotic agents such as azathioprine and mycophenolate mofetil, and calcineurin and mammalian target of rapamycin (mTOR) inhibitors. Monoclonal antibodies targeting T cells (CD3), activated T cells (IL2-R), myeloid cells (CD52), and dendritic cells (anti-B7 CTLA4 analogues), and polyclonal antilymphocyte preparations (antilymphocyte globulin, antithymocyte globulin) have each demonstrated efficacy to modulate various facets of the pathogenic alloimmune response. However, to date, none of the many combinations of these agents that have been applied in patients consistently prevents chronic rejection. Thus identification of a strategy to prevent chronic rejection is a high priority in transplant research.

Here we corroborate for what we believe is the first time in a preclinical solid organ allograft model that B cells exert a pivotal influence during the initiation of alloimmunity (14, 15, 20) by showing that their efficient depletion around the time of transplant is associated with significant protection from chronic rejection. This result confirms and extends findings in rodent heart transplant recipients (14) and a monkey islet allograft model (15) that B cells

A

B
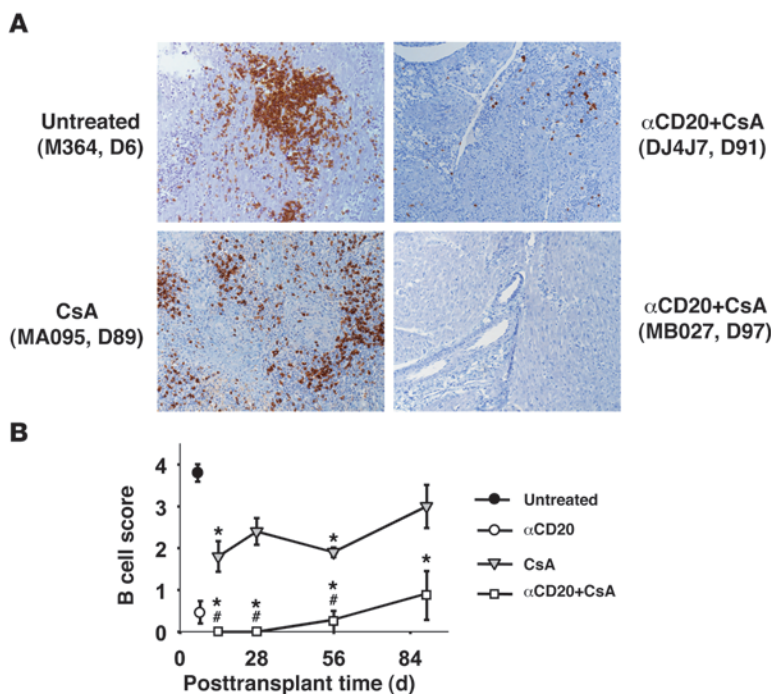
Figure 4
Immunochemistry analysis of graft-infiltrating B cells. Cardiac graft biopsy and explant tissue specimens were stained for CD20 and scored as described in Methods. (**A**) Representative pictures from explanted rejected (M364) or beating grafts (MA095, DJ4J7, MB027) demonstrate that effective perioperative B cell depletion by αCD20 treatment durably inhibits graft B cell infiltration (MB027), while partial recovery in peripheral blood correlates with B cell infiltrate in the graft (DJ4J7). (**B**) Quantitative B cell scores for αCD20+CsA, CsA, and untreated groups, expressed as mean ± SEM. Closed circle, untreated; open circle, αCD20 monotherapy; gray triangles, CsA; open squares, αCD20+CsA. $*P \leq 0.03$ vs. untreated controls; $^{\#}P \leq 0.03$ vs. CsA. Original magnification, ×100.

regulate nonredundant antigen-presenting functions previously ascribed mainly to other "professional" antigen-presenting cells during the initial response to alloantigen. Since B cell depletion has been used safely for other indications in oncology (21), autoimmunity (22), and in presensitized transplant patients (23, 24), this observation may facilitate an important clinical advance, one potentially broadly applicable to improving long-term results not only for heart allografts but for all transplanted organs.

Our observations support the working hypothesis that the efficiency and duration of B cell depletion is important to the observed effect of rituximab on alloantibody elaboration, graft infiltration by T cells, and CAV. The only rituximab-treated animal that exhibited incomplete initial B cell depletion and partial recovery of peripheral B cells by 2 months after transplant also was the only animal in this group that mounted a significant alloantibody response, associated with substantial C4d deposition, or whose graft contained a substantial population of B and T cells. Although the CAV score in this animal's graft was still low (0.33) at explant on day 91, our working model of CAV would predict a high probability of relatively rapid CAV progression in the context of alloantibody elaboration.

Elaboration of anti-donor antibody (25–29) and appearance of B cell–rich tertiary lymphoid structures (30–32) and expression of B cell genes in the graft (33, 34) are all closely associated with chronic rejection of the heart and other organ allografts in rodents, nonhuman primates, and human recipients. Our observations in the current study, that alloantibody detection, complement deposition, and CAV severity correlate closely with each other, add further compelling support for the generally accepted hypothesis that alloantibody contributes to the pathogenesis of CAV. Based on the large body of data suggesting that anti-donor antibody is pathogenic, depletion of B cells with rituximab (35, 36) and of plasma cells with bortezomib (37, 38) are being evaluated in kidney transplant patients. These studies will determine whether late posttransplant depletion of B cells or plasma cells will attenuate alloantibody production or modulate the progression of incipient chronic antibody-

mediated renal allograft rejection. However, the role of B cells in the initiation of acute and chronic rejection of a solid organ allograft has not previously been investigated in primates.

In our model, B cell depletion alone yields detectable but clinically insignificant prolongation of graft survival. In mice with intact immune systems receiving B cell–depleting reagents, CD4+ T cell responses to foreign and self antigens are significantly reduced, but CD8+ T cell activity is unaffected (20, 39, 40). B cell–deficient mice reject heart allografts with kinetics similar to WT controls (41–43), but with CsA, graft survival was significantly prolonged in μMT/μMT mice as compared with heterozygous controls (41). Russell et al. showed that both B cell–deficient and normal recipients developed cellular coronary endothelialitis, but sclerotic lesions did not progress in B cell–deficient mice, implicating alloantibody in progression but not initiation of CAV lesions (7). Noorchashm et al. engineered mice with a targeted deficiency of MHC class II–mediated Ag presentation confined to the B cell compartment (14). Cardiac allograft survival was markedly prolonged in these mice as compared with control counterparts (median survival time, >70 vs. 9.5 days), demonstrating that B cell APC function is pivotal to efficient induction of pathogenic alloimmunity.

A central role for B cells in the induction of alloimmunity could be explained by 2 nonexclusive mechanisms. First, B cell depletion radically alters the anatomy of primate secondary lymphoid organs (44). The architecture of this immune compartment and coordinated trafficking of various immunocytes through it are well known to dramatically influence the strength and phenotype of immune responses to allo-, auto-, and infectious antigens (45–48). Profound disruption of normal architecture following B cell depletion might therefore be expected to nonspecifically impair "protective" pathogenic responses to transplant antigens that depend on the cell-cell interactions and cytokines provided by this environment.

Secondly, B cells expressing high-affinity B cell receptors for allogenic peptide antigens not only give rise to plasma cells producing high-affinity anti-donor antibody, but also have recently
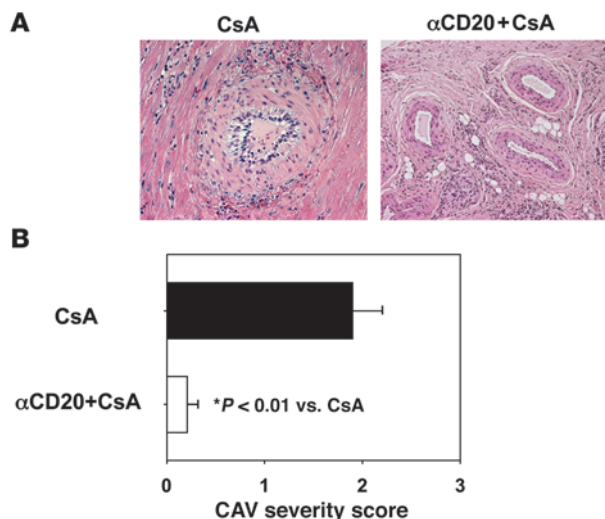
Figure 5
B cell depletion combined with CsA inhibits chronic cardiac allograft rejection. (**A**) Representative pictures from cardiac allografts explanted at approximately day 90 and stained with H&E. Vascular lesions of chronic rejection (intimal proliferation) are prominent with CsA monotherapy, but not with additional αCD20 treatment. Original magnification, ×200. (**B**) Quantitative CAV severity score is shown for explanted grafts from groups of animals treated with CsA or αCD20+CsA (mean ± SD).

been shown to be particularly efficient APCs (14, 17, 20). "Incidental" depletion of high-affinity donor-reactive B cells by rituximab eliminates an alloantigen-specific precursor population that is not only pivotal to efficient costimulation of high-affinity donor-reactive T cells, but which would otherwise evolve through classical immunoglobulin gene rearrangements to elaborate high-affinity anti-donor antibodies. This hypothesis would predict that subsequent repopulation of the periphery by donor antigen–specific B cell clones may prove pivotal to trigger acute or chronic rejection mechanisms. However, after profound selective B cell depletion, an environment that contains significant quantities of alloantigen during B cell recovery may facilitate deletion or anergy of high-affinity donor-specific B cell clones. Indeed, transient B cell depletion may promote the emergence of B cells with an altered repertoire or function that no longer triggers pathogenic responses, but promotes immune regulation (49–51) and even operational tolerance (15). This result may be particularly favored if the waves of B cell precursors that repopulate B cell niches from the bone marrow mature in the context of an immunologically quiescent (uninflamed) host, as exists months after the transplant procedure. Deletional tolerance and even "desensitization" to ABO carbohydrate antigens has been observed in a series of pediatric heart allograft recipients treated with conventional immunosuppression (52) and in adult recipients of other ABO-incompatible organ allografts treated with rituximab (53–57). The conditions under which responses to immunodominant transplant protein antigens may be durably regulated remain to be determined, as do the relative contribution of deletional, anergic, and immunomodulatory mechanisms.

Determining the contribution and relative importance of non–antigen-specific immune architecture disruption and antigen-specific mechanisms to the immunomodulatory effects of preemptive B cell depletion is not readily tractable using the limited tools

available in the primate model. Both mechanisms would predict relative depletion (limited expansion) of donor-specific Th or B cell clones. Unfortunately, the tetramer reagents needed to dissect out the number, phenotype, and functional characteristics of antigen-specific cells are available for only a few pathogen-associated antigens and a limited number of macaque histocompatibility antigens. Reconstitution of B cell–depleted animals with naive donor-reactive versus third-party–specific B cells at various time points after transplant is not feasible in monkeys. Nor are tools available to selectively interfere with lymphoid anatomy or to inhibit B and T cell function locally within various lymphoid compartments or in response to specific immunogenic donor antigens. Thus studies to dissect out the fundamental underlying mechanisms governing our observations and to test each of these hypotheses can best be accomplished in rodent transplant models.

In our experiments, CsA alone or with αCD20 tends to be associated with decreased pan-B (CD20, PAX5) and T cell (CD3E, CD28, IFN-γ [Th1], IL-17 [Th17]) graft mRNA expression when compared with acutely rejecting untreated grafts. Preemptive depletion of B cells is associated with significantly reduced proinflammatory T cell (Th1, Th17, TNF-α) and costimulatory (CD80, CD28) message 3 months after transplant, whereas Th2 cytokine and regulatory pathway genes are expressed at levels similar to those measured in an acutely rejecting graft. As a result, the cytokine balance in grafts from rituximab-treated animals is skewed toward a molecular phenotype (Th2 > Th1 or Th17) that has been associated with graft acceptance or tolerance in other models (57, 58). These data suggest that, unlike in other models (40, 59), normal B cell numbers are not required for Th2 differentiation after transplantation. While encouraging with respect to the tolerogenic potential of preemptive B cell depletion, the Th2 "regulatory" phenotype appears to be insufficient to prevent CAV in association with CsA treatment alone.

We previously reported that rituximab does not fully deplete B cells in the secondary lymphoid organs of a minority (1 of 4) of untransplanted nonhuman primates (44), a proportion similar to that observed in the current report. FcR polymorphisms have been described in humans that affect antibody-dependent cellular cytotoxicity (ADCC) function in response to rituximab (19, 60). Similar Fc-receptor polymorphisms may exist in monkeys. Low cell-surface CD20 receptor density, CD20 polymorphisms that attenuate rituximab-binding affinity, and relative B cell resistance to ADCC are less likely alternative explanations for reduced B cell depletion efficiency with rituximab in a minority of treated monkeys.

The majority of the animals in the αCD20+CsA group had persistent depletion of peripheral blood B cells to 10% or less of pretreatment levels through this study's predefined 3-month study end point. Further studies will be needed to determine how subsequent reconstitution of germinal centers and partial recovery of peripheral blood B cell numbers, as is often seen clinically, influences anti-donor alloantibody elaboration and CAV. Whether B cell–targeted induction will facilitate safer steroid or calcineurin inhibitor–sparing immunosuppressive regimens also remains to be determined.

We found that rituximab was well tolerated in cynomolgus monkeys that were additionally immunosuppressed with a calcineurin inhibitor. Except for 1 animal that was euthanized for anemia due to a parvovirus infection, rituximab- and CsA-treated heart allograft recipients appeared healthy and exhibited resilience in the context of multiple surgical procedures (graft biopsies and explant, regular phlebotomy). The safety, efficacy, and side effect
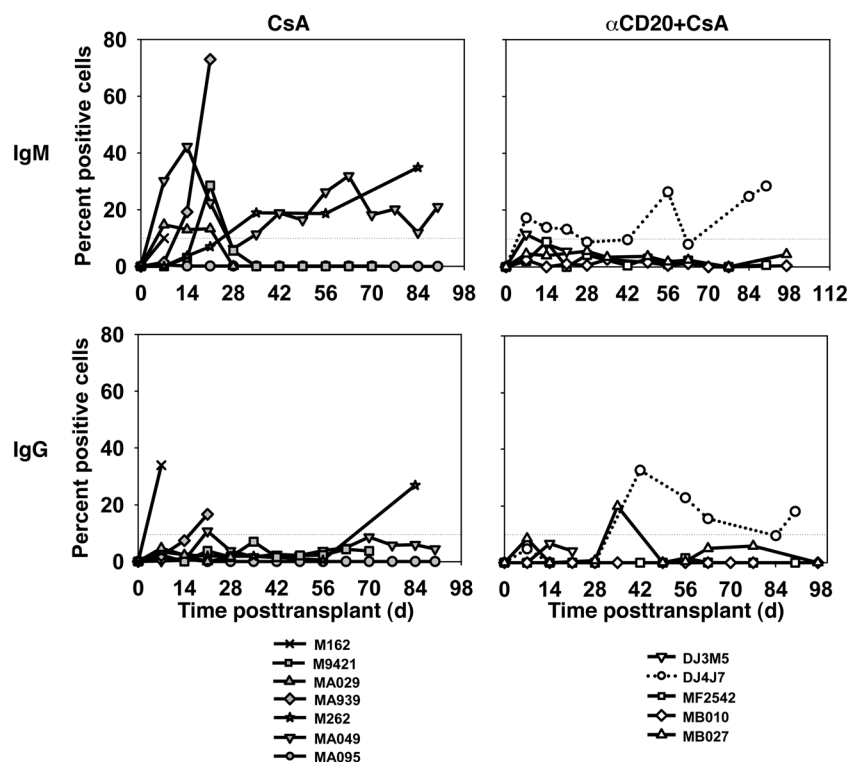
Figure 6
B cell depletion is associated with inhibition of alloantibody production. IgM (upper panels) and IgG (lower panels) anti-donor antibodies were detected by flow cytometry in serum from most CsA-treated animals (left panels) (5/7 for IgM, 3/7 for IgG). With addition of αCD20 (right-hand panels), IgM and IgG were consistently detected (>10% limit of detection sensitivity on more than one occasion) only in the animal that exhibited less durable B cell depletion in peripheral blood (DJ4J7, dotted line).

profile of rituximab in human studies have been well established in patients with B cell lymphoma (21). We have previously reported that reactivation of latent parvovirus may be associated with and attributable to immunosuppression. However, death of MA939 cannot necessarily be ascribed to the αCD20+CsA regimen, since acute primary parvovirus infection can prove lethal even in the absence of pharmacologic immunosuppression (61). Liu et al. have shown that memory humoral immune responses to tetanus immunization are intact months after B cell depletion in operationally tolerant islet recipients, suggesting that B cell depletion per se does not significantly impair protective immunity in the long term (15). Further investigation is needed to evaluate de novo and recall (secondary) immune responses to vaccines and clinical infections both acutely and over longer term follow-up after rituximab administration and particularly when used in conjunction with other clinical immunosuppressants.

In our estimation, significant inhibition of CAV associated with preemptive B cell depletion justifies a clinical trial of depleting B cells around the time of an organ transplant, even if the mechanisms have not yet been definitively established. Based on our findings, we predict that preemptive B cell depletion will attenuate both T and B cell–mediated pathogenic immunity and delay or prevent chronic rejection in those patients who exhibit efficient, sustained B cell clearance. Further, our work suggests that monitoring B cell recovery in the periphery will identify nonresponders, who are likely at increased risk for acute rejection and CAV.

In summary, our work shows that the immune response to an allograft is particularly susceptible to B cell depletion at a proximal point in the kinetics of the immune response, confirming and extending similar findings in a nonhuman primate intraportal islet transplant model (15). Until a clinically feasible approach to specifically target donor-reactive B cells can be devised (62), pre-emptive "induction" CD20+ B cell depletion represents a clinically applicable strategy to delay or potentially prevent anti-donor alloantibody elaboration and CAV.

Methods

Cynomolgus monkeys. Captive-bred and wild-caught cynomolgus monkeys (*Macaca fascicularis*) were utilized for this study. All procedures were approved by the institutional animal care and use committee at the University of Maryland School of Medicine and were conducted in compliance with NIH guidelines for the care and use of laboratory animals. Males and females weighing 2.8–5.5 kg were selected as organ recipients of ABO blood type–compatible donors of either sex. Stimulation index of greater than 3 assured that each donor-recipient pair was MHC class II–mismatched, and pairings were arranged so as to maximize mixed lymphocyte reaction response within groups of blood type–compatible animals (median 18, range 5.8–73).

Surgical procedure. All recipient animals underwent heterotopic intraabdominal cardiac transplantation, as described previously (10, 17). Graft function (electrocardiogram voltage; left ventricular systolic and diastolic pressure; heart rate) and core temperature were assessed by telemetry (D70-PCTP, Data Sciences International; implanted at the time of transplantation) at least once daily until graft explant. Acute rejection was typically heralded by fever (>38°C after the first postoperative week). Signs of graft failure included intraventricular pressure wave form damping and diminished graft heart rate (<140 beats per minute or a decline >20% from that recipient's stable postoperative baseline heart rate) and were seen with both acute and chronic rejection. Grafts were also monitored by palpation or transabdominal ultrasound during times when animals were chemically restrained for blood draws (1–3 times weekly) or if there was evidence by telemetry of graft dysfunction. Primary graft failure was defined as symptomatic acute rejection, diagnosed by at least 2 of 3 signs (fever, decreased heart rate, decreased graft pulse pressure); primary graft failure due to
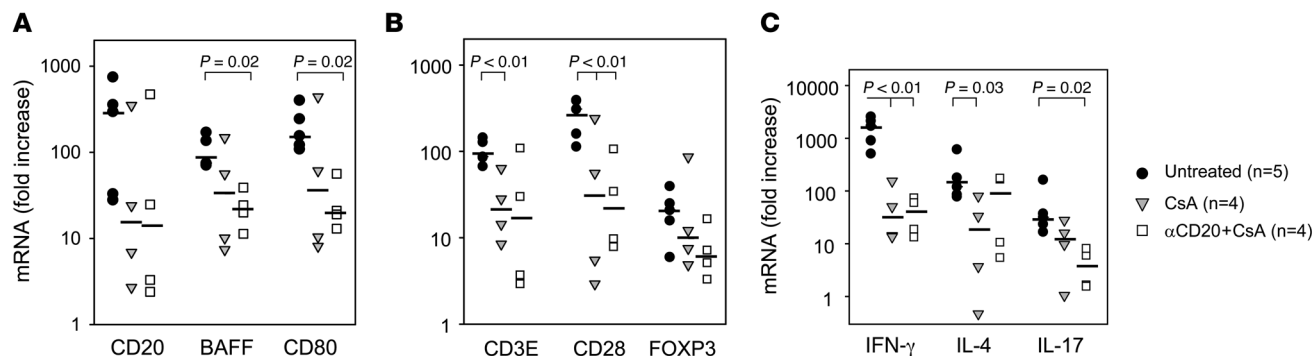
Figure 7
Intragraft gene expression in explanted cardiac allografts. Relative expression levels of B cell (**A**), T cell (**B**), and T-lineage–related cytokine genes (**C**) by real-time RT-PCR demonstrate a trend toward decreased B and T cell gene expression in association with additional peritransplant B cell depletion, with a bias away from Th17 and toward Th2 (IL-4). DJ4J7 accounts for the highest value for each B cell marker in part **A**. Expressed as a ratio of proinflammatory T cell cytokine genes (IFN-γ+TNF-α+IL-17) to FOXP3 gene expression, overall T cell inflammation was suppressed similarly with CsA or αCD20+CsA, without evidence for a regulatory bias with additional αCD20 ($P < 0.02$ versus untreated; data not shown). The black bar displays the group median, while each symbol represents an individual animal. Missing values reflect absence of high-quality mRNA for 2 animals in the CsA group. P values are reported for comparisons where values of less than 0.05 were calculated.

chronic rejection (gradual graft failure without fever) was not observed in the current study. When diagnosed, acute rejection was treated with methylprednisolone (40 mg/kg i.v. once followed by 20 mg/kg daily for 2 days; cat. no. 9086745, Solu Medrol, Henry Schein). Secondary graft failure was defined as loss of telemetric, palpable, and visible graft activity after previous steroid treatment. Open cardiac biopsies were performed by protocol on postoperative days 14 and 28 and monthly thereafter until graft explant whenever clinical condition allowed. Grafts were explanted at the time of failure or at the protocol end point of 3 months (85–96 days).

Experimental groups and drug immunosuppression dosing. Recipients that received no immunosuppression (*n* = 5) were included as a reference group as previously reported (17). Thirteen animals received CsA (cyclosporine injectable, cat. no. 1100667; Henry Schein) initiated at a dose of 15 mg/kg i.m. daily. Trough CsA levels were checked 1 to 2 times weekly and the daily dose (5–22.5 mg/kg) adjusted to a target trough level between 400 and 600 ng/ml until the time of graft explant. Five recipients also received chimeric anti-CD20 antibody (rituximab [Rituxan], gift of Genentech; αCD20), 20 mg/kg i.v. the day before transplantation and on postoperative days 7, 14, and 21; 2 additional recipients were treated with this rituximab regimen, but without cyclosporine (αCD20 alone). The efficiency of this regimen to deplete peripheral blood and secondary lymphoid tissue B cells in this species has been described previously (44).

Blood sampling and flow cytometry staining of peripheral lymphocytes. Cell blood counts (CBC) and B and T lymphocyte subsets were measured by protocol at regular intervals in freshly collected EDTA blood using an automated cell counter (Hemavet) and flow cytometry, respectively. All antibodies used for flow cytometry were obtained from BD Biosciences — Pharmingen. Because anti-human CD20 antibody (clone 2H7) competes for binding with rituximab, B cells were identified among viable leukocytes as CD3⁻ (clone SP34), CD14⁻ (clone M5E2), and DR⁺ (clone L243). (Direct staining with clone 2H7 in normal monkey PBL consistently validated the accuracy of this approach.) Briefly, 100 µl of fresh blood was incubated with appropriate antibodies for 20 minutes at 4°C, and red blood cells were lysed with BD FACSLyse. Data analysis and graphic display were conducted using CellQuest or WinList software. The proportion of B or T lymphocytes in the leukocyte population was multiplied by absolute counts of white blood cells from the CBC analysis to calculate absolute B and T lymphocyte counts per µl of blood.

Detection of anti-donor alloantibody. Alloantibodies were measured retrospectively by flow cytometry using archived frozen donor splenocytes and recipient serum as described previously (10, 63). Antibody binding was revealed using PE-labeled goat anti-human IgM (Fcμ specific) antibodies (Biosource) or biotin-labeled goat anti-monkey IgG (Fcγ specific) antibodies (Nordic) followed by PE-labeled streptavidin (BD Biosciences — Pharmingen). FITC-labeled anti-human CD3 (BD Biosciences — Pharmingen) was added to gate on T cells. Alloantibody reactivity was defined as an increase of more than 10% in the proportion of IgM- or IgG-positive donor cells relative to donor serum before transplant. Anti-donor antibodies were not measured in 1 CsA group animal (M115) because viable donor cells were not available.

Histology and CAV quantification. Biopsy and explant tissue specimens were fixed with 10% formalin and processed routinely for paraffin embedding. Sections of paraffin-embedded tissue were stained with H&E. Classification of cellular infiltrates was done according to ISHLT criteria for acute allograft rejection (18). CAV severity was scored in all explanted hearts that survived beyond 40 days. Three independent evaluators (S.S. Kelishadi, T. Zhang, and R.N. Pierson III) blinded with respect to treatment group evaluated a minimum of 20 and up to 50 epicardial arteries and intramyocardial arterioles by morphology on H&E and elastin stain in multiple levels from each explant. CAV was graded as follows: grade 0, normal arterial morphology; grade 1, activated endothelial cells with enlarged nuclei and/or adherent leukocytes and with less than 10% luminal narrowing; grade 2, distinct neointimal thickening and luminal narrowing of 10%–50%; and grade 3, extensive neointimal proliferation with more than 50% luminal occlusion. The CAV severity score for each explant was calculated using the following equation: (no. grade 1 vessels) × 1 + (no. grade 2 vessels) × 2 + (no. grade 3 vessels) × 3/total number of arterial vessels scored. After unblinding, the mean of the 3 independent CAV measurements was accepted as the score for that sample. Individual graft mean CAV scores were averaged to calculate the group mean (±SD) for each treatment group.

Immunohistochemistry for quantification of B cells. IHC staining for B cells was performed using an automated method as follows. Formalin-fixed paraffin-embedded tissue sections were deparaffinized and stained on the Ventana ES Automated Stainer (Ventana Medical Systems Inc.) using mouse anti-human CD20 antibody (L26; DAKO) and the ABC method (Ventana reagents, and mild CC1, conditioner 1 and standard 1 settings). The stain-

ing of B cells was verified by a pathologist (C. McMahon) and scored by one investigator (A.M. Azimzadeh) blinded with respect to treatment group using the following scale: 0, absence of B cells; 1, scattered focal staining or weak diffuse B cell infiltrate; 2, 1–3 discrete B cell–rich nodules or mild diffuse infiltrate; 3, 3–10 nodules or moderately intense diffuse infiltrate; 4, more than 10 nodules or intense diffuse infiltrate.

Real-time RT-PCR. Heart tissue specimens were snap-frozen in liquid nitrogen and stored at –70°C. Total RNA was isolated from cardiac grafts using the RNeasy Mini Kit from QIAGEN. Briefly, tissue was disrupted in RLT buffer, digested with proteinase K, loaded on columns, and treated with DNase I (QIAGEN). Purified RNA was quantified and assessed for purity and integrity by capillary electrophoresis using the Agilent Bioanalyzer. cDNA was generated from 3 to 6 μg of each RNA sample using SuperScript II RNase H–reverse transcriptase (Invitrogen) and a mix of oligo (dT) and random primers in the ratio of 4:1 (Applied Biosystems and Invitrogen). 60 ng of the resultant cDNA was used in each PCR reaction. HPRT1 was chosen as housekeeping gene control after testing the relative expression of a panel of normal and rejected monkey heart samples. Primers and TaqMan probes used are listed in Supplemental Table 1. The real-time PCR assay was performed on the ABI Prism 7900 (Applied Biosystems). The expression of each gene was normalized to HPRT1 using the $\Delta\Delta C_T$ calculation. mRNA levels were finally expressed as relative fold increase over normal monkey heart (average of 4 individual normal native heart tissue samples). Gene expression was not measured in 3 CsA group animals because RNA was degraded (M115, M162) or frozen tissue not available (M9421).

C4d staining. Tissue deposits of C4d were assayed using double-fluorescence immunochemistry on OCT frozen tissue sections as previously described (63). The presence of C4d was scored by 2 investigators (A.M. Azimzadeh and R.N. Pierson III) blinded with respect to treatment group using the following scale: 0, absence of staining; 0.5, less than 10% vessels positive; 1, 10%–20% vessels positive; 2, 20%–50% vessels positive; 2.5, more than 50% vessels positive. If capillary staining was also present, the vessel score was increased by 0.5 points.

Statistics. Continuous variables (CAV score, gene expression) were expressed as the mean + SD unless otherwise indicated and were compared using the Mann-Whitney nonparametric test. Graft survival time was graphed using the Kaplan-Meier method, and the log-rank test was used to compare survival time between groups. Nominal variables (incidence of early rejection or alloantibody production) were compared using a contingency table and the Fischer exact test. P values less than 0.05 were considered statistically significant. All statistical analyses were performed on a personal computer with the statistical package SPSS for Windows XP (version 11.0; SPSS) or GraphPad InStat (version 5.1; GraphPad software).

1. Sheashaa HA, et al. Long-term evaluation of basiliximab induction therapy in live donor kidney transplantation: a five-year prospective randomized study. *Am J Nephrol*. 2005;25(3):221–225.

2. Ciancio G, Burke GW III. Alemtuzumab (Campath-1H) in kidney transplantation. *Am J Transplant*. 2008;8(1):15–20.

3. Kumar A, et al. Comparison of four different immunosuppression protocols without long-term steroid therapy in kidney recipients monitored by surveillance biopsy: five-year outcomes. *Transpl Immunol*. 2008;20(1–2):32–42.

4. Pierson RN III, et al. Thoracic organ transplantation. *Am J Transplant*. 2004;4(Suppl 9):93–105.

5. Leichtman AB, et al. Kidney and pancreas transplantation in the United States, 1997-2006: the HRSA Breakthrough Collaboratives and the 58 DSA Challenge. *Am J Transplant*. 2008;8(4 Pt 2):946–957.

6. Mulligan MS, et al. Heart and lung transplantation in the United States, 1997–2006. *Am J Transplant*. 2008;8(4 Pt 2):977–987.

7. Russell PS, Chase CM, Colvin RB. Alloantibody- and T cell–mediated immunity in the pathogenesis of transplant arteriosclerosis: lack of progression to sclerotic lesions in B cell–deficient mice. *Transplantation*. 1997;64(11):1531–1536.

8. Gleit ZL, et al. Persistent chimerism despite anti-donor MHC in vitro responses in miniature swine following allogeneic hematopoietic cell transplantation. *Transplantation*. 2002;74(9):1260–1266.

9. Smith RN, et al. Four stages and lack of stable accommodation in chronic alloantibody-mediated renal allograft rejection in Cynomolgus monkeys. *Am J Transplant*. 2008;8(8):1662–1672.

10. Azimzade AM, et al. Alloimmunity in primate heart recipients with CD154 blockade: evidence for alternative costimulation mechanisms. *Transplantation*. 2006;81(2):255–264.

11. Baker RJ, et al. Loss of direct and maintenance of indirect alloresponses in renal allograft recipients: implications for the pathogenesis of chronic allograft nephropathy. *J Immunol*. 2001;167(12):7199–7206.

12. Reed EF, et al. Monitoring of soluble HLA alloantigens and anti-HLA antibodies identifies heart allograft recipients at risk of transplant-associated coronary artery disease. *Transplantation*. 1996;61(4):566–572.

13. Itescu S, et al. An immunological algorithm to predict risk of high-grade rejection in cardiac transplant recipients. *Lancet*. 1998;352(9124):263–270.

14. Noorchashm H, Greeley SA, and Naji A. The role of t/b lymphocyte collaboration in the regulation of autoimmune and alloimmune responses. *Immunol Res*. 2003;27(2–3):443–450.

15. Liu C, et al. B lymphocyte-directed immunotherapy promotes long-term islet allograft survival in non-human primates. *Nat Med*. 2007;13(11):1295–1298.

16. Bour-Jordan H, Bluestone JA. B cell depletion: a novel therapy for autoimmune diabetes? *J Clin Invest*. 2007;117(12):3642–3645.

17. Schröder C, et al. CCR5 blockade modulates inflammation and alloimmunity in primates. *J Immunol*. 2007;179(4):2289–2299.

18. Stewart S, et al. Revision of the 1990 working formulation for the standardization of nomenclature in the diagnosis of heart rejection. *J Heart Lung Transplant*. 2005;24(11):1710–1720.

19. Smith MR. Rituximab (monoclonal anti-CD20 antibody): mechanisms of action and resistance. *Oncogene*. 2003;22(47):7359–7368.

20. Crawford A, Macleod M, Schumacher T, Corlett L, Gray D. Primary T cell expansion and differentiation in vivo requires antigen presentation by B cells. *J Immunol*. 2006;176(6):3498–3506.

21. Winter MC, Hancock BW. Ten years of rituximab in NHL. *Expert Opin Drug Saf*. 2009;8(2):223–235.

22. Remuzzi G, Chiurchiu C, Abbate M, Brusegan V, Bontempelli M, Ruggenenti P. Rituximab for idiopathic membranous nephropathy. *Lancet*. 2002;360(9337):923–924.

23. Vo AA, et al. Rituximab and intravenous immune globulin for desensitization during renal transplantation. *N Engl J Med*. 2008;359(3):242–251.

24. Becker YT, Becker BN, Pirsch JD, Sollinger HW. Rituximab as treatment for refractory kidney transplant rejection. *Am J Transplant*. 2004;4(6):996–1001.

25. Vongwiwatana A, Tasanarong A, Hidalgo LG, Halloran PF. The role of B cells and alloantibody in the host response to human organ allografts. *Immunol Rev*. 2003;196:197–218.

26. Colvin RB, Smith RN. Antibody-mediated organ-allograft rejection. *Nat Rev Immunol*. 2005;5(10):807–817.

27. Tarlinton DM, Batista F, Smith KG. The B-cell response to protein antigens in immunity and transplantation. *Transplantation*. 2008;85(12):1698–1704.

28. Kwun J, Knechtle SJ. Overcoming chronic rejection — Can it B? *Transplantation*. 2009;88(8):955–961.

29. Terasaki PI, Cai J. Human leukocyte antigen antibodies and chronic rejection: from association to causation. *Transplantation*. 2008;86(3):377–383.

30. Kayler LK, et al. Acute cellular rejection with CD20-positive lymphoid clusters in kidney transplant patients following lymphocyte depletion. *Am J Transplant*. 2007;7(4):949–954.

31. Obhrai JS, et al. Effector T cell differentiation and memory T cell maintenance outside secondary lymphoid organs. *J Immunol*. 2006;176(7):4051–4058.

32. Baddoura FK, Nasr IW, Wrobel B, Li Q, Ruddle NH, Lakkis FG. Lymphoid neogenesis in murine cardiac allografts undergoing chronic rejection. *Am J Transplant*. 2005;5(3):510–516.

33. Zarkhin V, Li L, Sarwal M. "To B or not to B?" B-cells and graft rejection. *Transplantation*. 2008;85(12):1705–1714.

34. Scherer A, et al. Transcriptome changes in renal allograft protocol biopsies at 3 months precede the onset of interstitial fibrosis/tubular atrophy (IF/TA) at 6 months. *Nephrol Dial Transplant*. 2009;24(8):2567–2575.

35. Study of rituximab to treat chronic renal transplant rejection (RituxiCAN-C4). London, United Kingdom: King's College London; 2009. URL: http://clinicaltrials.gov/ct2/show/NCT00476164. Accessed January 26, 2010.

36. B-Cell depletion by anti-CD20 (Rituximab) in renal allograft recipients who develop early de novo anti-HLA alloantibodies. Bethesda, MD: NIAID; 2007. URL: http://clinicaltrials.gov/ct2/show/NCT00307125. Accessed January 26, 2010.

37. The impact of velcade (TM) on antibody secreting cells in sensitized renal allograft candidates. Rochester, MN: Mayo Clinic; 2009. URL: http://clinicaltrials.gov/ct2/show/NCT00722722. Accessed January 26, 2010.

38. Everly JJ, Walsh RC, Alloway RR, Woodle ES. Proteasome inhibition for antibody-mediated rejection. *Curr Opin Organ Transplant*. 2009;14(6):662–666.

39. Liu Q, et al. The role of B cells in the development of CD4 effector T cells during a polarized Th2 immune response. *J Immunol*. 2007;179(6):3821–3830.

40. Moulin V, Andris F, Thielemans K, Maliszewski C, Urbain J, Moser M. B lymphocytes regulate dendritic cell (DC) function in vivo: increased interleukin 12 production by DCs from B cell-deficient mice results in T helper cell type 1 deviation. *J Exp Med*. 2000;192(4):475–482.

41. Brandle D, Joergensen J, Zenke G, Burki K, and Hof RP. Contribution of donor-specific antibodies to acute allograft rejection: evidence from B cell-deficient mice. *Transplantation*. 1998;65(11):1489–1493.

42. Alexander DZ, Pearson TC, Hendrix R, Ritchie

SC, Larsen CP. Analysis of effector mechanisms in murine cardiac allograft rejection. *Transpl Immunol*. 1996;4(1):46–48.

43. Nozaki T, Rosenblum JM, Ishii D, Tanabe K, Fairchild RL. CD4 T cell-mediated rejection of cardiac allografts in B cell-deficient mice. *J Immunol*. 2008;181(8):5257–5263.

44. Schroder C, Azimzadeh AM, Wu G, Price JO, Atkinson JB, Pierson RN. Anti-CD20 treatment depletes B-cells in blood and lymphatic tissue of cynomolgus monkeys. *Transpl Immunol*. 2003;12(1):19–28.

45. Lakkis FG, Arakelov A, Konieczny BT, Inoue Y. Immunologic 'ignorance' of vascularized organ transplants in the absence of secondary lymphoid tissue. *Nat Med*. 2000;6(11):686–688.

46. Ochando JC, et al. Lymph node occupancy is required for the peripheral development of alloantigen-specific Foxp3+ regulatory T cells. *J Immunol*. 2005;174(11):6993–7005.

47. Weyand CM, Kang YM, Kurtin PJ, Goronzy JJ. The power of the third dimension: tissue architecture and autoimmunity in rheumatoid arthritis. *Curr Opin Rheumatol*. 2003;15(3):259–266.

48. Junt T, Scandella E, Ludewig B. Form follows function: lymphoid tissue microarchitecture in antimicrobial immune defence. *Nat Rev Immunol*. 2008;8(10):764–775.

49. Bouaziz JD, Yanaba K, Tedder TF. Regulatory B cells as inhibitors of immune responses and inflammation. *Immunol Rev*. 2008;224:201–214.

50. Deng S, et al. Cutting edge: transplant tolerance induced by anti-CD45RB requires B lymphocytes. *J Immunol*. 2007;178(10):6028–6032.

51. Monach PA, Schreiber H, Rowley DA. CD4+ and B lymphocytes in transplantation immunity. II. Augmented rejection of tumor allografts by mice lacking B cells. *Transplantation*. 1993;55(6):1356–1361.

52. Fan X, et al. Donor-specific B-cell tolerance after ABO-incompatible infant heart transplantation. *Nat Med*. 2004;10(11):1227–1233.

53. Pierson RN III, et al. Successful management of an

ABO-mismatched lung allograft using antigen-specific immunoadsorption, complement inhibition, and immunomodulatory therapy. *Transplantation*. 2002;74(1):79–84.

54. Just SA, et al. Acute antibody-mediated rejection after ABO-incompatible kidney transplantation treated successfully with antigen-specific immunoadsorption. *Nephrol Dial Transplant*. 2010;25(1):310–313.

55. Ikegami T, et al. Rituximab, IVIG, and plasma exchange without graft local infusion treatment: a new protocol in ABO incompatible living donor liver transplantation. *Transplantation*. 2009;88(3):303–307.

56. Ichimaru N, Takahara S. Japan's experience with living-donor kidney transplantation across ABO barriers. *Nat Clin Pract Nephrol*. 2008;4(12):682–692.

57. Strom TB, et al. The Th1/Th2 paradigm and the allograft response. *Curr Opin Immunol*. 1996;8(5):688–693.

58. Chen N, Gao Q, Field EH. Prevention of Th1 response is critical for tolerance. *Transplantation*. 1996;61(7):1076–1083.

59. Liu Q, et al. The role of B cells in the development of CD4 effector T cells during a polarized Th2 immune response. *J Immunol*. 2007;179(6):3821–3830.

60. Weng WK, Levy R. Two immunoglobulin G fragment C receptor polymorphisms independently predict response to rituximab in patients with follicular lymphoma. *J Clin Oncol*. 2003;21(21):3940–3947.

61. Schroder C, et al. Simian parvovirus infection in cynomolgus monkey transplant recipients causes death related to severe anemia. *Transplantation*. 2006;81(8):1165–1170.

62. Kirk AD, et al. American society of transplantation symposium on B cells in transplantation: harnessing humoral immunity from rodent models to clinical practice. *Am J Transplant*. 2007;7(6):1464–1470.

63. Azimzadeh AM, et al. Humoral immunity to vimentin is associated with cardiac allograft injury in nonhuman primates. *Am J Transplant*. 2005;5(10):2349–2359.